A Modeling and Evaluation of the Random Telegraph Signal Noise on a CMOS Image Sensor in Motion Pictures

Deng Zhang, *Hiroaki Ammo, Jegoon Ryu, *Hirofumi Sumi, and Toshi Hiro Nishimura
Graduate school of Information, Production and Systems, WASEDA University,
SONY Corporation*
2-7 Hibikino, Watamatsu-ku, Kitakyuushyuu, 808-0135 Japan, 4-14-1, Asahi-cho, Atsugi, Kanagawa, 243-0014 Japan*
zhdnstar@fuji.waseda.jp, tosi-hiro@waseda.jp

Abstract—**This paper presents a motion picture simulator with the newly proposed Random Telegraph Signal (RTS) noise model. Different from traditional researches on RTS noise, it is concerned primarily with the noise source distribution on a CMOS image sensor (CIS) instead of a single pixel in this work. Besides, a new video quality evaluation method for RTS noise on CIS in motion pictures is developed, which is named as RTS Video Quality (RTS_VQ). Using this simulator with RTS_VQ, the sensory rating of CIS imaging with RTS noise is obtained by our video quality evaluation method.**

Keywords-CMOS Image Sensor, Random Telegraph Signal Noise, Video Quality

I. INTRODUCTION

It is a trend to produce high quality images and videos by cameras in the near future as increasing perceptual requirement of human, in which high quality images and videos are defined as high resolution and hardly any noise. However, as the downscaling of the pixel to achieve high resolution, Random Telegraph Signal (RTS) noise is becoming pronounced and brings heavily perceptual impact of videos. And a RTS noise is the discrete changes in drain current resulting from carrier trapping and de-trapping into single oxide defect and appears as a fluctuation in the voltage. A typical two level RTS noise is shown in Fig. 1, where $\tau_{u,s}$ and $\tau_{d,p}$ are the s-th duration and the p-th duration of an impulse in the up and down time respectively; ΔI is the amplitude of the RTS noise.

Until now, a part of the mechanism of RTS noise on CIS has been reported, but most of the previous works on RTS noise have mainly focused on the characteristics of a RTS noise in a single CIS pixel either in time domain, i.e. Probability Density Function (PDF) [1]-[3], or in the frequency domain, i.e. Power Spectra Density (P.S.D) function [1], [3]-[5]. At the same time, all the results given in these works are based on physical experiments on MOS devices. And highly effort would be required to ones who study RT noise mechanism and noise reduction using computer. So, mathematics is significantly required for the precise noise modeling of RTS noise.

Reducing the RTS noise, which we mentioned, pictures aiming at high quality videos are much demanded. The most effective method based on the precise RTS noise modeling in CIS is much demanded today. Nevertheless, because to remove the single oxide defect in the surface of MOSFET is extremely difficult and the cost of it increases proportionately to the number of pixels that need be de-defected, the effort of RTS noise sources cancelation comes up as one of the most significant problems in CIS manufacturing process. Therefore, CIS manufacturing have to cancel RTS noise source as much as possible on the premise of that the distortion of video could be barely perceptible. With this view, an effective video quality evaluation method is demanded to provide a reference of the distortion videos to them in order to estimate the degree of distortion introduced by RTS noise in a motion picture.

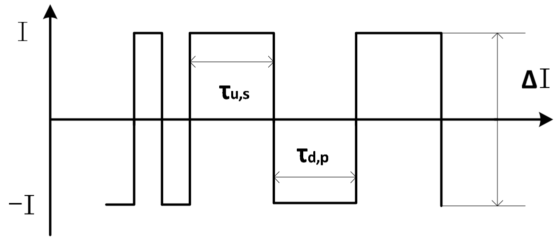

Figure 1. A typical two-level RTS noise

The often calculated video quality evaluation method is Peak Signal-to-noise Ratio (PSNR) based on mean square error (MSE), which is somewhat a mean value and does not agree with the RTS noise case.

In order to solve the problems mentioned above, we firstly developed a video camera exposure simulator (VCES) with the newly proposed RTS noise modeling on CIS in motion picture. Based on the analysis of the proposed noise model, we propose a novel video quality evaluation method named as RTS Video Quality (RTS_VQ). Finally, conclusions about the RTS noise model and the effectiveness of RTS_VQ can be drawn from the numerical experimental results.

II. METHODOLOGY

The VCES is developed to simulate the noise generation in the exposure process of a video camera and based on the newly proposed RTS noise mode consisting of a Gaussian component

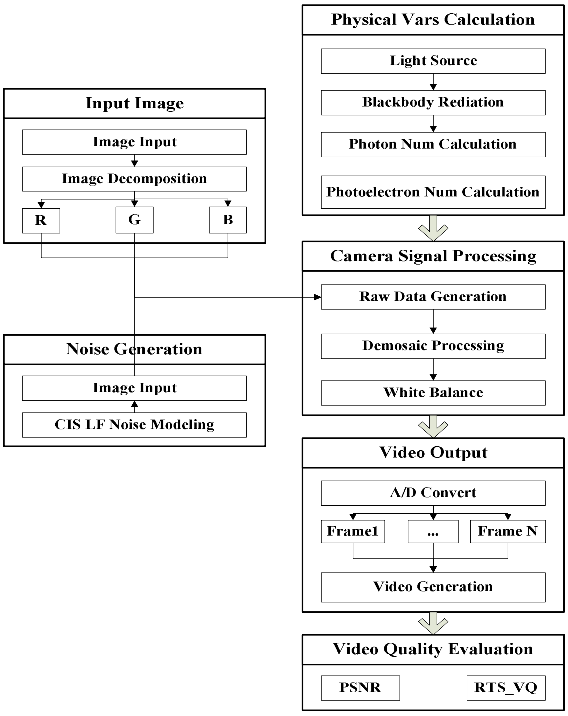

Figure 2. Flowchart of VCES

noise and a non-Gaussian component noise, and this newly proposed RTS noise model already includes the conventional 1/f noise. The flowchart of VCES is shown in Fig .2 and the noise free frame used in VCES is Macbeth chart shown in Fig. 3 [6]-[9].

A. RTS Noise Model

In this paper quantities noise level and noise histogram are proposed to quantificationally describe the RTS noise situation in a single CIS pixel and on a CIS respectively. In VCES dark current shot noise and dark current Fixed Pattern Noise (FPN), thermal noise, reset noise, 1/f noise, and light FPN are modeled as the Gaussian component noise. The number of pixels at a noise level x $P_{Norm}(x)$is given as (1),

$$P_{Norm}(x) = K \times \frac{1}{\sqrt{2\pi\sigma}} e^{-\frac{(x-\mu)^2}{2\sigma^2}} \quad (1)$$

where K is a coefficient related to the total pixel number of a CIS, x is noise level in Digital Number (DN); μ and σ are the mean and standard deviation of the Gaussian component noise

Figure 3. Noise free Macbeth chart

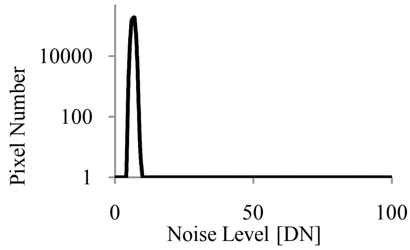

Figure 4. Noise Histogram of the Gaussian component noise

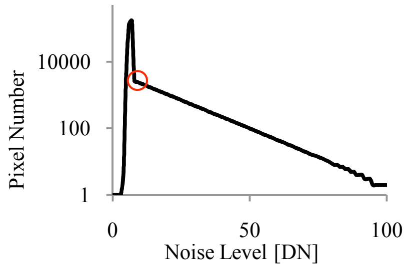

Figure 5. Noise Histogram of the Gaussian component noise and the non-Gaussian component noise

by means of curve fitting. The noise histogram of Gaussian component is shown in Fig. 3, where the vertical and horizontal axes represent P_{Norm} and noise level respectively.

In VCES, the non-Gaussian component noise refers to a typical two-level RTS noise as shown in Fig. 1. This non-Gaussian component noise model is based on the work in [10]-[16] and determined by a two-parameter A and B exponential distribution. And the number of pixels at a noise level x $P_{RTS}(x)$ is given as (2),

$$P_{RTS}(x) = Ae^{-Bx} \quad (2)$$

where parameters A and B are coefficients related to the scale and the shape parameter of the spatial distribution of RTS noise sources respectively, and x represents noise level. Actually the RTS noise amplitudes of different pixels at a same noise level follow a Gaussian distribution N ~ (μ_2, σ_2). And the noise histogram slightly dithers as the value of σ_2 changes.

The noise histogram of the newly proposed RTS noise model is shown in Fig. 4 and (2)-(5) are used to construct such a noise histogram,

$$P_{Norm1}(x) = K_1 \times \frac{1}{\sqrt{2\pi\sigma_1}} e^{-\frac{(x-\mu_1)^2}{2\sigma_1^2}} \quad (3)$$

$$\sum_{x=0}^{N} P_{Norm}(x) = \sum_{x=0}^{C_x} P_{Norm1}(x)$$
$$+\sum_{x=C_x+1}^{N} P_{RTS}(x) \quad (4)$$

$$P_{Norm1}(C_x) = P_{RTS}(C_x) \quad (5)$$

where $P_{Norm1}(x)$ is the number of pixels only with the Gaussian component noise at noise level x, K_1, σ_1, and μ_1 has the same meaning with K , σ, and μ in (2); N is the maximum noise level on a CIS, and C_x is the x-coordinate of the connected point marked by a red circle.

B. Evaluation Method

RTS_VQ is a metric to evaluate the perceptual impact of video distortions introduced by RTS noise and is developed to reflect the relationship between the video quality and the spatial distributions of RTS noise sources on a CIS. Since the number of pixels with single oxide defect which is RTS noise source is very small compared with the total number of pixels of a CIS, the values of PSNR are identical for motion pictures even if they have quite different distortion situations. On the contrary, RTS_VQ emphasizes the effect of larger noise level and makes use of the characteristics of the spatial distribution of RTS noise on a CIS. The definition of RTS_VQ is given as (6)-(8),

$$meanDist = \sqrt{meanR^2 + meanG^2 + meanB^2} \quad (6)$$

$$maxDist = 10 \times \sqrt{\begin{matrix}(maxR \times slopeR)^2 + \\ (maxG \times slopeG)^2 + \\ (maxB \times slopeB)^2\end{matrix}} \quad (7)$$

$$RTS\_VQ = meanDist + 0.005 \times maxDist \quad (8)$$

where meanDist is the mean distortion of the video; meanR, meanG, and meanB are mean distortion of R, G and B channels; maxDist is the maximum distortion of the video; maxR, slopeR, maxG, slopeG, maxB, and slopeB are maximum distortion and slope of R, G and B channels respectively; 0.005 is weight parameter of the maximum distortion and is chosen based on several primitive psychophysics experiments. All the noise histograms are in log-scale, in that way the minority RTS noise source relative to the total CIS pixel number contributes much more to the value of RTS_VQ than its original value.

III. Numerical Experiments

VCES in numerical experiments is analogous to a physical video camera, and parameters configuration of them are similar and given in Table I. The output of VCES is a motion picture with 30 frames per second, in which a frame is a 480 × 720 Macbeth chart. The simulation results of Macbeth chart with the proposed RTS noise model are shown in Fig. 6.

As shown in Table I, the size of a CIS pixel in VCES is 2µm × 2µm which is a submicron MOSFET device pronounced by a RTS noise. In order to test the proposed RTS noise model, five different noise situations, Case 0 – Case 5 (explained in Table II) are defined with changing the values of parameters A, B, and σ_2, where Case 0 is defined as only the Gaussian component noise is included and Case 1-4 include both the Gaussian component noise and the RTS noise. The noise histograms Case 1-4 are shown in Fig. 7

To demonstrate the effectiveness of RTS_VQ, both the

Table I. Configuration of VCES

Parameter	Value	Parameter	Value
Focus	4	**Intensity**	320
ISO	200	**Shutter Speed**	0.004s
Pixel Pitch	2 µm	**Color Temp**	5500K
Sensor Temperature	300K	**σ_2 (default)**	2.0

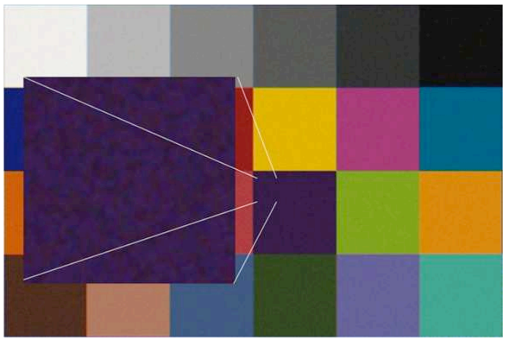

(a) Only Gaussian component noise

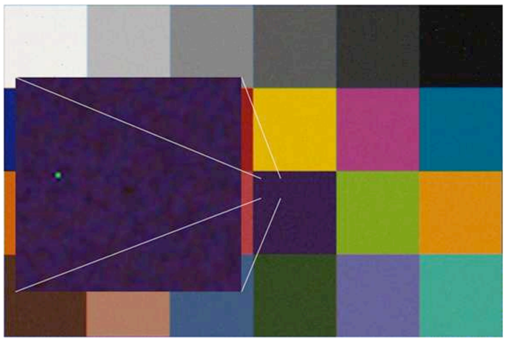

(b) Gaussian component noise and RTS noise

Figure 6. Simulation results of Macbeth chart within two different noise conditions with the proposed RTS noise model

values of PSNR and RTS_VQ for Case 0-5 are both calculated and shown in Table II.

We have a small area of the noisy Macbeth charts enlarged to amplify the impact of noise on an image. Fig. 6 (a) shows some irregular streaks caused by the Gaussian component noise, and in Fig. 6 (b), a prominent spot appears which is caused by RTS noise with large noise level. Further, it is shown from the result motion pictures that flickers caused by RTS noise affects human visual sensitivity significantly as the value of RTS_VQ increases, which could also be reflected by the noise histogram changing in Fig. 8. As shown in Fig. 7 (a) and (c), the Case 1 and the Case 3 have the same values of parameter B but the different values of A. Correspondingly, the straight downward-sloping lines of the noise histograms in Fig. 7 (a) and (c) have same shape but different scale. So are the Case 2 and the Case 4 in Fig. 7 (b) and (d). Comparatively, the Case 1 and the Case 2 shown in Fig. 7 (a) and (b) respectively have the same values of parameter A but the different values of B, which results in totally different shape of noise histograms. And the Case 2 and the Case 4 in Fig. 7 (b) and (d) are in the same way.

As the results of PSNR and RTS_VQ for Case 1-4 shown in Table II, PSNR remains identical as expected as the value of parameter A decreases or the value of parameter B increases, whereas RTS_VQ can evaluate the video distortion introduced by RTS noise more efficient. It is also shown in Table II that RTS_VQ decreases indicating worse video quality when σ_2 decreases resulting from that RTS noise with large amplitude appears. Especially, the noise histogram of σ_2 0.5 is more fitting to the physical experimental results than 2.0.

Table II. PSNR and RTS_VQ values for four RTS noise situations

Noise Conditions	RTS noise parameter		C_x	$\sigma_2 = 2.0$		$\sigma_2 = 0.5$	
	A	*B*		*PSNR*	*RTS_VQ*	*PSNR*	*RTS_VQ*
Case 0	—	—	—	14.38	13.25	14.38	13.25
Case 1	5000	0.0782	9	14.38	22.91	14.38	21.97
Case 2	5000	0.2482	10	14.38	15.64	14.38	15.53
Case 3	1000	0.0782	10	14.38	21.24	14.38	21.08
Case 4	1000	0.2482	10	14.38	14.73	14.38	14.64

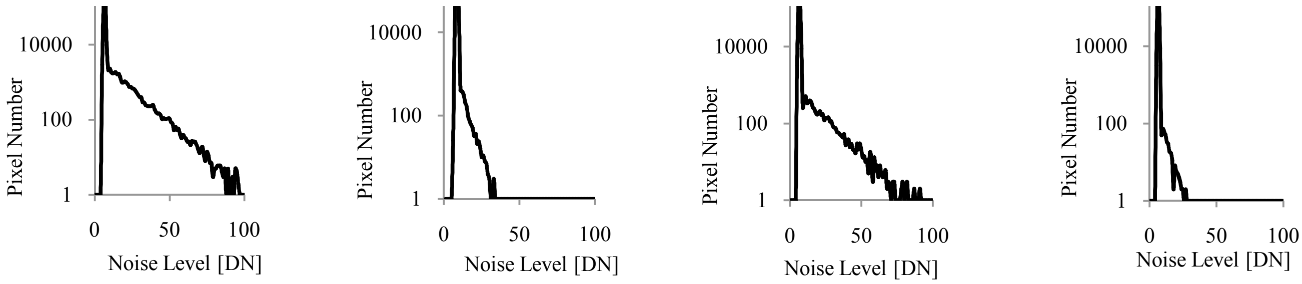

(a) Case 1 (b) Case 2 (c) Case 3 (d) Case 4

Figure 7. Noise histogram of Case 1-4 in Table II from (a) to (d)

IV. CONCLUSION

A high quality motion picture with quantificational analysis of RTS noise is obtained based on those works mentioned above. Eventually, we will draw our conclusions that RTS noise becomes less significant as the value of parameter A decreases or parameter B increases shown in Table II. The flickers caused by RTS noise more significantly affect the human visible sensation as RTS_VQ increasing, while PSNR remains almost identical.

At last, because there is only a marginal difference of the values of RTS_VQ and PSNR between Case 0, Case 2 and Case 4, which means the video distortion degree is applicable to CIS manufacturers to control the value of RTS noise source cancellation since they have not to motivate a noise histogram like Case 0.

The authors greatly appreciate to Mr. Kazuyuki Matsushima, Mr. Hiroaki Katsuma and Dr. Ing. Kazuhiro Hoshino, the Nishimura Laboratory of Waseda University.

REFERENCES

[1] J.S. Kolhatkar, E.Hoekstra, C.Salm, "Modeling of RTS Noise in MOSFETs under Steady-State and Large-Signal Excitation," 2004, IEEE.

[2] G.Ghibaudo, T.Boutchacha, "Electrical noise and RTS fluctuations in advanced CMOS devices," Microelectronics Reliability 42 (2002).

[3] Alicja Konczakowska, Jacek Cichosz, Arkadiusz Szewczyk, "A New Method for RTS Noise of Semiconductor Devices Identification," IEEE Tran. ON Instrumentation and Measurement.

[4] Arnoud P. van der Wel, Eric A. M. Klumperink, L. K. J. Vandamme, and Bram Nauta "Modeling Random Telegraph Noise Under Switched Bias Conditions Using Cyclostaionary RTS Noise," IEEE Trans. Electron Devices, vol. 50, n0. 5, May 2003.

[5] Cédric Leyris, François Roy, Mathieu Marin "Modeling of the temporal pixel to pixel noise of CMOS image sensors," 2007 International Image Snsor Workshop.

[6] Danny Pascale, "RGB coordinates of the Macbeth colorchecker," 1st June 2006, www.Babel.com, pp. 1-16.

[7] Jun-yan Huo, Yi-lin Chang, Jing Wang, and Xiao-xia Wei "Robust Automatic White Balance Algorithm using Gray Color Points in Images," 2006 IEEE.

[8] Y. Kim, H. S. Lee, A.W. Morales, "A video camera system with enhanced zoom tracking and auto white balance," IEEE Trans. Consumer Electron, vol.48, no. 3, pp. 428-434, Aug. 2002.

[9] Y. Liu, W. Chan and Y. Chen, "Automatic white balance for digital still camera," IEEE Tran. Consumer Electron, vol.41, no. 3, pp. 460-466, Aug. 1998.

[10] K.Abe, S. Sugawa, S. Watabe, N. Miyamoto ,A. Teramoto, Y. Kamata, K. Shibusawa, M. Toita4 and T. Ohmi "Random Telegraph Signal Statistical Analysis using a Very Large-scaleArray TEG with 1M MOSFETs," 2007 Symposium on VLSI Technology Digest of Technical Papers, Jun., 2007, 210-211.

[11] Xinyang Wang, Padmakumar R. Rao, Adri Mierop*, Albert J.P. Theuwissen "Random Telegraph Signal in CMOS Image Sensor Pixels," International Electron Device Meeting 200.6.

[12] C. Leyris, S. Pilorget, M. Marin, M. Minondo, H. Jaouen, "Random Telegraph Signal Noise SPICE Modeling for Circuit Simulators," 2007 IEEE.

[13] C. Leyris, J-C. Vildeuil, F. Roy, F. Martinez, M. Valenza, A. Hoffmann "Response of Correlated Double Sampling CMOS Imager Circuit to Random Telegraph Signal Noise," the 6th International Caribbean Conference on Devices, Circuits and Systems, Mexico, Apr. 26-28, 2006.

[14] K. Abe, T. Fujisawa, A. Teramoto, S. Watabe, S. Sugawa, and T. Ohmi, "Anomalous RTS Extractions from a Very Large Number of n-MOSFETs using TEG with 0.47 Hz – 3.0 MHz Sampling Frequency," Extended Abstracts of the 2008 International Conference on Solid State Devices and Materials, Tsukuba, 2008, pp. 888-889.

[15] Shigetoshi Sugawa, "Random Telegraph Signal noises in small MOS devices," IEICE Tech. Rep., vol. 108, no. 253, ICD2008-75, pp. 95-100, Oct. 2008.

[16] Shigetoshi Sugawa, Kenichi Abe, Takafumi Fujisawa, Shunichi Watabe, Rihito Kuroda, Naoto Miyamoto, "Statistical Analyses of Random Telegraph Signals in the TransistorsEquivalent to Pixel Source Fo llowers Us ing aL arge-scale Array TEG," ITE Technical Report Vo I. 32 , No.19 , PP.9~12, IST 2008-10, CE 2008-23.